Tuning conventional non-TADF units to high-lying reverse intersystem crossing TADF emitters: a symmetric D–A–D type modified different donor units

Xue Bai,[a] Shui-xing Wu,[b] Ying-chen Duan,[a] Qing-qing Pan,[a] Feng-wei Gao,*[ac] Yu-he Kan,*[d] Zhong-min Su *[ae]

[a] School of Chemistry and Environmental Engineering, Changchun University of Science and Technology, 7989 Weixing Road, Changchun 130012, China.

[b] Laboratory of Electrochemical Energy Storage and Energy Conversion of Hainan Province, School of Chemistry & Chemical Engineering, Hainan Normal University, Haikou 571158, China.

[c] Chongqing Research Institute, Changchun University of Science and Technology, No.618 Liangjiang Avenue, Longxing Town, Yubei District, Chongqing City 401135, China.

[d] Jiangsu Province Key Laboratory for Chemistry of Low-Dimensional Materials, School of Chemistry and Chemical Engineering, Huaiyin Normal University, Huai'an 223300, China.

[e] State Key Laboratory of Supramolecular Structure and Materials, Institute of Theoretical Chemistry，College of Chemistry, Jilin University, Changchun 130021, China.

E-mail: gaofw@cust.edu.cn, kyh@hytc.edu.cn, zmsu@nenu.edu.cn

Table of contents

Table S1. Dihedral angle (°) between the donor and the acceptor at optimized S_0, S_1 and T_1 States, together with their differences (Δ) at the CAM- B3LYP/6-31G(d) level 2

Table S2. Overlap integrals of norm and centroid distances (Å) between the HOMO and LUMO pairs 3

Table S3. Calculated singlet and triplet excitation energy levels (eV) for PTZ-MPS, TPA-MPS and PCz-MPS with their optimal ω values at the LC-ωPBE/6-31G(d) level 4

Table S4. SOC matrix elements $\langle S_1 | \hat{H}_{SOC} | T_n \rangle$ at S_1 state of all molecules 5

Figure S1. Hole−electron pairs of NTOs in S_1 to S_5 and T_1 to T_5 of PTZ-MPS. The hole wavefunctions are below the electron wavefunctions 6

Figure S2. Hole−electron pairs of NTOs in S_1 to S_5 and T_1 to T_5 of TPA-MPS. The hole wavefunctions are below the electron wavefunctions 7

Figure S3. Hole−electron pairs of NTOs in S_1 to S_5 and T_1 to T_5 of PCz-MPS. The hole wavefunctions are below the electron wavefunctions 8

Table S1. Dihedral angle (°) between the donor and the acceptor at optimized S_0, S_1 and T_1 states, together with their differences (Δ) at the CAM- B3LYP/6-31G(d) level

	Dihedral angle	S_0	S_1	**Δ** (S_1- S_0)	T_1	**Δ** (T_1- S_0)
PTZ-MPS	C1-N2-C3-C4	83.65	93.51	9.86	83.42	-0.23
TPA-MPS	C1-C2-C3-C4	36.24	38.38	2.14	36.99	-0.75
PCz-MPS	C1-C2-C3-C4	38.58	38.26	-0.32	40.33	2.04

Table S2. Overlap integrals of norm and centroid distances (Å) between the HOMO and LUMO pairs

	PTZ-MPS	**TPA-MPS**	**PCz-MPS**
Overlap integrals	0.164	0.500	0.342
Centroid distances (Å)	2.70	3.49	5.23

Table S3. Calculated singlet and triplet excitation energy levels (eV) for PTZ-MPS, TPA-MPS and PCz-MPS with their optimal ω values at the LC-ωPBE/6-31G(d) level

	ω	S_1	S_2	S_3	S_4	S_5	T_1	T_2	T_3	T_4	T_5
PTZ-MPS	0.1731	2.98	2.98	3.39	3.40	3.68	2.81	2.81	2.95	2.96	3.27
TPA-MPS	0.1640	3.52	3.64	3.74	3.74	4.00	2.80	2.82	3.20	3.20	3.37
PCz-MPS	0.1704	3.84	3.91	3.99	4.00	4.32	3.11	3.12	3.25	3.33	3.33

Table S4. SOC matrix elements $<S_1 | \hat{H}_{soc} | T_n>$ at S_1 state of all molecules

$<S_1 \| \hat{H}_{soc} \| T_n>$ at the S_1 geometry			
	PTZ-MPS	**TPA-MPS**	**PCz-MPS**
T_1	0.0356	0.1917	0.3851
T_2	0.0328	0.1423	0.1831
T_3	1.0131	0.3107	0.3537
T_4	0.8938	0.5857	0.1019
T_5	0.5766	0.2306	0.1008

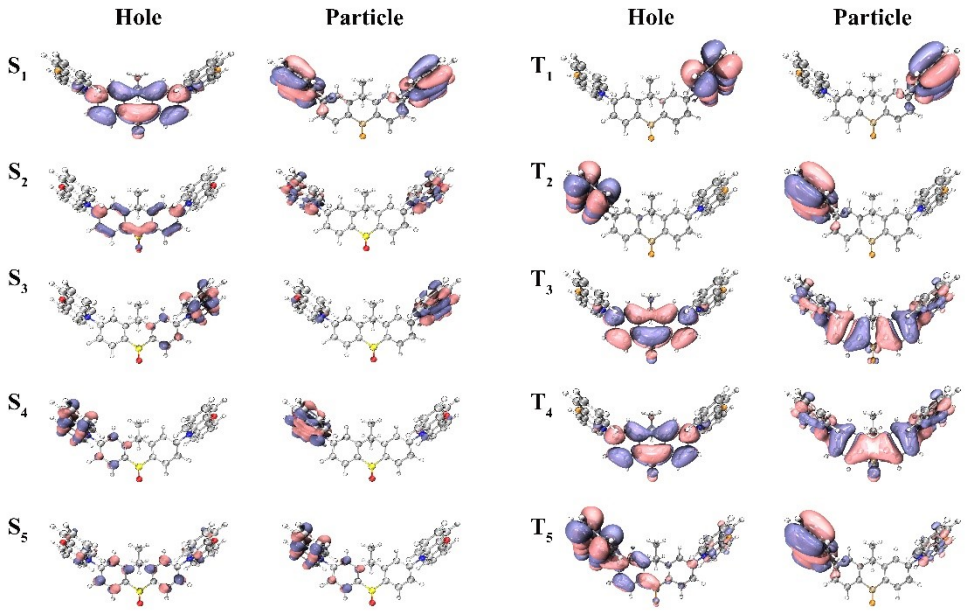

Figure S1. Hole−electron pairs of NTOs in S_1 to S_5 and T_1 to T_5 of PTZ-MPS. The hole wavefunctions are below the electron wavefunctions

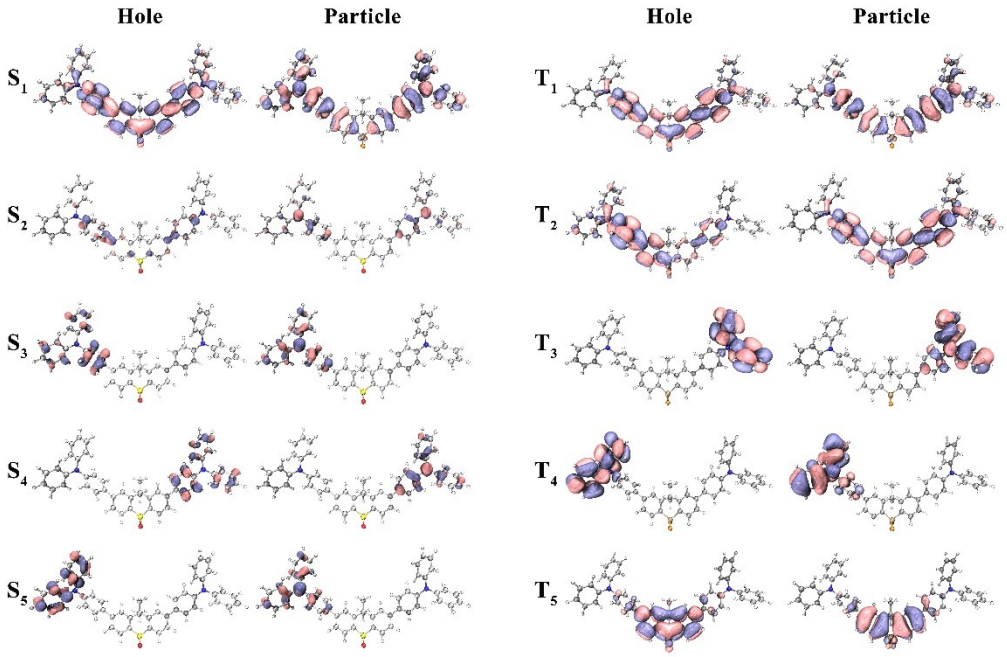

Figure S2. Hole−electron pairs of NTOs in S_1 to S_5 and T_1 to T_5 of TPA-MPS. The hole wavefunctions are below the electron wavefunctions

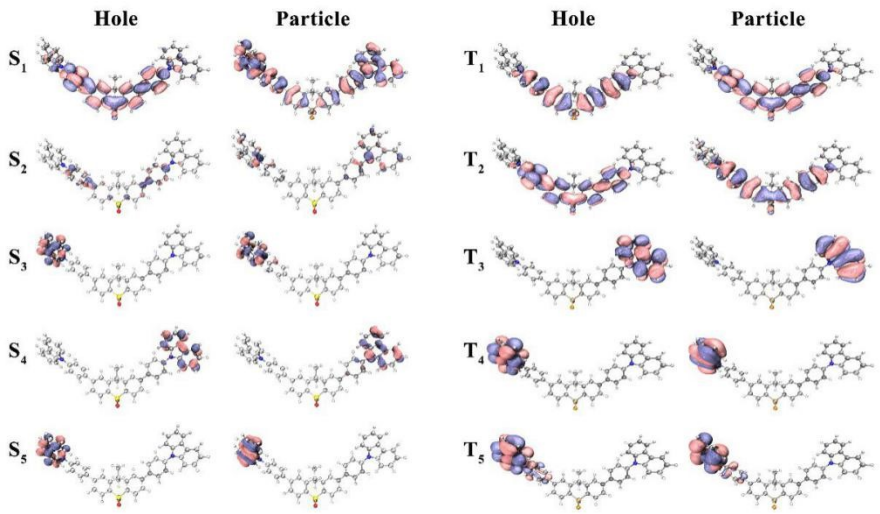

Figure S3. Hole−electron pairs of NTOs in S_1 to S_5 and T_1 to T_5 of PCz-MPS. The hole wavefunctions are below the electron wavefunctions